Desynchronization waves in small-world networks

Kwangho Park and Liang Huang
Department of Electrical Engineering, Arizona State University, Tempe, Arizona 85287, USA

Ying-Cheng Lai
Department of Electrical Engineering, Arizona State University, Tempe, Arizona 85287, USA and Department of Physics and Astronomy, Arizona State University, Tempe, Arizona 85287, USA

(Received 16 November 2005; revised manuscript received 6 November 2006; published 21 February 2007)

A regular array of oscillators with random coupling exhibits a transition from synchronized motion to desynchronized but ordered waves as a global coupling parameter is increased, due to the spread of localized instability of eigenvectors of the Laplacian matrix. We find that shortcuts, which make a regular network small-world, can destroy ordered desynchronization wave patterns. Wave patterns in a small-world network are usually destroyed gradually as the degree of regularity in the network deteriorates. No ordered wave patterns are observed in scale-free and random networks. The formation of ordered wave patterns in a coupled oscillator network can be explained by considering the time evolution of phase in each oscillator. We derive a general type of the Kardar-Parisi-Zhang equation for phase evolution in a prototype oscillator network. The equation demonstrates well the ordered desynchronized wave patterns found in the network with and without shortcuts. Our results provide a qualitative justification for the requirement of certain degree of regularity in the network for ordered wave patterns to arise.

DOI: 10.1103/PhysRevE.75.026211 PACS number(s): 05.45.Xt, 05.10.−a, 89.75.−k

I. INTRODUCTION

Synchronization in complex networks is a topic of growing recent interest [1–7]. Usually, one is concerned with the synchronizability of networks with the small-world [8–12] or the scale-free [9–13] topology, which can be analyzed by the master-stability function approach [14]. In particular, given a complex network, one can make it "dynamic" by placing an oscillator on each node, effectively generating an oscillator network. The complex-network topology can be conveniently described by a coupling matrix, the Laplacian matrix. The stability of a synchronized solution can be analyzed by solving the variational equations in all eigensubspaces transverse to the synchronization manifold. In each subspace, the effective coupling parameter is proportional to the eigenvalue of the Laplacian matrix associated with this subspace. The master stability function is the largest transverse Lyapunov exponent that determines the maximal exponential rate of growth of a small perturbation from the synchronization manifold. Physically meaningful synchronization requires that this function be negative. Typically, for an oscillator network, the master-stability function can be negative only in a finite interval, say (K_1,K_2), of some normalized coupling parameter K. Since the range of K is determined by the spread of the eigenvalues of the Laplacian matrix, the network synchronizability can be characterized by this spread. To our knowledge, most existing works focused almost exclusively on the interplay between the network topology and synchronizability [1–7].

In this paper, we go beyond the synchronizability issue by focusing on desynchronization wave patterns in complex networks. In many fields where synchronization is important [15], such as biology [16], laser physics [17], and chemistry [18], etc., the emergence of wave patterns is an interesting issue. One can imagine a synchronized oscillator network, where no wave appears due to the synchronized motion of all oscillators. Wave patterns can arise when desynchronization occurs, say, due to a change in the coupling parameter. Thus desynchronization is a physical mechanism through which wave patterns can be generated in the underlying network. In this regard, the recent work by Restrepo *et al.* [19] investigated, for *regular* oscillator networks with random coupling, how desynchronization wave patterns may be generated as the normalized coupling parameter K falls outside the synchronization interval (K_1,K_2). Their finding is that ordered wave patterns can be generated as a result of the propagation of the Anderson localization of some unstable eigenmodes. Considering that under noise and/or oscillator parameter mismatches, a *stable* system can exhibit irregular desynchronization bursts, the presence of more ordered wave patterns in the locally *unstable* system is remarkable.

The question that we wish to address here is how the complex-network topologies may affect the desynchronization wave pattern. We first focus on a regular network and then consider random shortcuts, that make the network small-world (SW) [8], and further investigate complex networks with random and scale-free structure where regularity does not exist. Our main result is that ordered wave patterns in a SW network are destroyed gradually as the number of random shortcuts increases, i.e., as the degree of regularity in the network deteriorates. Considering that such shortcuts generally make the network more synchronizable [1,2], our finding that in the locally unstable system the role of shortcuts is the opposite is surprising. Our numerical efforts on scale-free and random networks reveal no ordered wave patterns. We find that the deterioration of ordered wave patterns in SW networks can be explained theoretically by considering the time evolution of the phase of each oscillator in the network. We derive a general type of Kardar-Parisi-Zhang (KPZ) equation for the evolution. The equation is capable of

generating wave patterns that are observed in direct numerical simulations. Our results suggest that desynchronized wave patterns in general cannot occur in complex networks with no local regularity in their connectivities.

In Sec. II, we investigate the effect of complex-network topology on desynchronized wave patterns through numerical simulations of four different network structures and show that desynchronized wave patterns appear only in networks with certain degree of regularity. In Sec. III, we derive a dynamic equation for phase evolution in a prototype SW oscillator networks. The partial differential equation can reproduce wave patterns observed in numerical simulations. A brief conclusion is presented in Sec. IV.

II. OSCILLATOR NETWORKS AND DESYNCHRONIZED WAVE PATTERN

We begin with a prototype of oscillator network: a ring network with periodic boundary conditions [19]. Each oscillator, when isolated, is described by $d\mathbf{x}/dt=\mathbf{F}(\mathbf{x})$, where $\mathbf{x}$ is a d-dimensional vector and $\mathbf{F}(\mathbf{x})$ is the velocity field. Since we are interested in wave patterns, we choose the parameters in $\mathbf{F}(\mathbf{x})$ such that it generates periodic oscillations of period T (i.e., a periodic attractor). For concreteness, we choose the Rössler oscillator so that $\mathbf{x}=[x,y,z]^t$ and $\mathbf{F}(\mathbf{x})=[-(y+z),x+0.2y,0.2+z(x-2.5)]^t$, where $[*]^t$ denotes the transpose. The equations describing the dynamics of a ring network of N nodes are

$$\frac{d\mathbf{x}_i}{dt}=\mathbf{F}(\mathbf{x}_i)-g\sum_{j=1}^{N}G_{ij}\mathbf{H}(\mathbf{x}_j),\quad i=1,\ldots,N, \tag{1}$$

where the index i denotes the spatial location of the ith oscillator on the ring, g is a global coupling parameter, G_{ij}'s are the elements of the symmetric Laplacian matrix that satisfy $\Sigma_j G_{ij}=0$, and $\mathbf{H}(\mathbf{x})=[x,0,0]^t$ is a linear coupling function (chosen somewhat arbitrarily). To model random coupling, the matrix elements G_{ij} are drawn from a uniform distribution in the interval [0.1,1.0] so that no value of the matrix element is small enough to effectively disconnect the network. The explicit form of the Laplacian matrix is

$$G=\begin{pmatrix} b_1 & -a_1 & 0 & 0 & \cdots & 0 & -a_N \\ -a_1 & b_2 & -a_2 & 0 & \cdots & 0 & 0 \\ 0 & -a_2 & b_3 & -a_3 & \cdots & 0 & 0 \\ \vdots & \vdots & \vdots & \vdots & \vdots & \vdots & \vdots \\ -a_N & 0 & 0 & 0 & \cdots & -a_{N-1} & b_N \end{pmatrix}, \tag{2}$$

where $b_i=(a_{i-1}+a_i)$. Adding a shortcut between node i and j is equivalent to setting $G_{ij}=G_{ji}=\alpha_i$, where α_i is a random number from [0.1,1.0]. To keep the coupling matrix Laplacian, we adjust the diagonal matrix element b_i so that the property $\Sigma_j G_{ij}=0$ always holds when shortcuts are added to the network. The matrix's being Laplacian makes a linear stability analysis of the synchronization state feasible, as Eq. (1) permits an exact synchronized solution: $\mathbf{x}_1(t)=\mathbf{x}_2(t)=\cdots=\mathbf{x}_N(t)=\mathbf{s}(t)$, where $d\mathbf{s}/dt=\mathbf{F}(\mathbf{s})$ and $\mathbf{s}(t+T)=\mathbf{s}(t)$. The variational equations governing the time evolution of the set of infinitesimal vectors $\boldsymbol{\delta}x_i(t)\equiv\mathbf{x}_i(t)-\mathbf{s}(t)$ are

$$\frac{d\delta\mathbf{x}_i}{dt}=\mathbf{DF}(\mathbf{s})\cdot\delta\mathbf{x}_i-g\sum_{j=1}^{N}G_{ij}\mathbf{DH}(\mathbf{s})\cdot\delta\mathbf{x}_j, \tag{3}$$

where $\mathbf{DF}(\mathbf{s})$ and $\mathbf{DH}(\mathbf{s})$ are the Jacobian matrices of the corresponding vector functions evaluated at $\mathbf{s}(t)$. Diagonalizing the Laplacian matrix G yields a set of eigenvalues $0=\lambda_1<\lambda_2\leqslant\cdots\leqslant\lambda_N$ and the associated eigenvectors $\mathbf{e}_1,\mathbf{e}_2,\ldots,\mathbf{e}_N$. The transform $\delta\mathbf{x}=\delta\mathbf{y}\cdot O^t$, where O is the orthogonal matrix whose columns are the set of eigenvectors, leads to the block-diagonally decoupled form of Eq. (3): $d\delta\mathbf{y}_i/dt=[\mathbf{DF}(\mathbf{s})-g\lambda_i\mathbf{DH}(\mathbf{s})]\cdot\delta\mathbf{y}_i$. Letting $K=g\lambda_i$ $(i=2,\ldots,N)$ be the normalized coupling parameter, we can write

$$\frac{d\delta\mathbf{y}}{dt}=[\mathbf{DF}(\mathbf{s})-K\mathbf{DH}(\mathbf{s})]\cdot\delta\mathbf{y}. \tag{4}$$

The largest Lyapunov exponent from Eq. (4) is the master-stability function $\Psi(K)$ [14].

For the chosen periodic Rössler oscillator, the function $\Psi(K)$ is negative in the interval $[0^+,K_c]$, where $K_c\approx4.15$ [19]. Thus, for $K<K_c$, all eigenvectors (eigenmodes) are transversely stable and the network is synchronized. Unstable eigenmodes begin to arise as K is increased through K_c, leading to desynchronization. For the regular ring-network configuration, for $K\gtrsim K_c$ the unstable eigenmodes are exponentially localized in space and these are the "triggers" of ordered desynchronization wave patterns [19]. For instance, for $g=1.3(\lesssim g_c)$ and $N=500$, the six eigenmodes associated with the six largest eigenvalues are unstable and the remaining 494 eigenmodes are stable. For $g>g_c$, where g_c depends on network structure, the network becomes unstable. Because of the periodic motion of each Rössler oscillator, it is insightful to examine its phase variable, which can be conveniently defined as

$$\varphi(i,t)\equiv 2\pi\frac{n(i,t)+[t-t_-(i,t)]}{[t_+(i,t)-t_-(i,t)]},$$

where $t_-(i,t)=\max\{s:x_i(s)=0,\dot{x}_i>0,s\leqslant t\}$, $t_+(i,t)=\min\{s:x_i(s)=0,\dot{x}_i>0,s>t\}$, and $n(i,t)$ is an integer chosen so that φ is a continuous function of t and that $\varphi(i+1,t)$ is close to $\varphi(i,t)$ for all i. Starting from the synchronized state, say $\mathbf{x}_i(0)=0$ and $\varphi(0)=0$, arbitrarily small perturbations to $\mathbf{x}_i(0)$ induce localized unstable eigenmodes, which spread the instability to nearby and then to distant nodes through coupling, eventually leading to an ordered wave pattern, as shown by the snapshots of φ_i and x_i at three instants of time in Fig. 1. The locations of the six localized unstable eigenmodes are visible in Figs. 1(d) and 1(f). The orderedness of the desynchronization wave pattern can be assessed by the nearly smooth variations of both the phase and the dynamical variables over the network, as can be seen in Figs. 1(e) and 1(f).

When shortcuts are added to the network, the eigenvalues shift in the eigensubspace, leading to a shift in the critical global coupling parameter g_c. We observe that the ordered desynchronization wave pattern deteriorates and is appar-

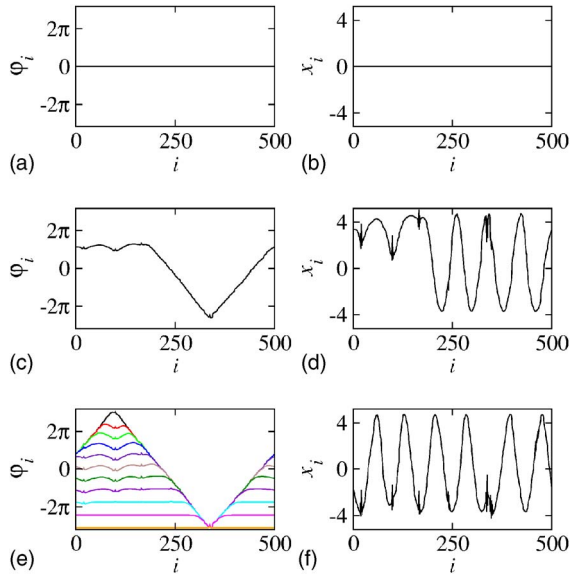

FIG. 1. (Color online) Snapshots of the phase variables $\varphi_i(t)$ and the dynamical variables $x_i(t)$ over the network introduced in Eq. (1): (a, b) $t=0$, (c, d) $t=5600$, (e) $t=11\,200$, 7700, 7000, 6300, 5600, 4900, 4200, 3500, 2800, 2100, and 1400 from top to bottom, and (f) $t=11\,200$. From (e), we see that phase surface becomes rougher with time for $t<\tau(\approx 10\,000)$, but the trend stops for $t>\tau$, where a facet morphology is formed at $t=\tau$. From (d, f), we see that for large times, the dynamical variables $x_i(t)$ exhibit nearly regular and smooth spatial variations over the network, indicating an ordered wave pattern. The spatially localized unstable eigenmodes can be identified by the small spikes on top of the smooth variation of x_i.

ently destroyed when the number of shortcuts, M, is increased, as shown in Fig. 2. In this case, an analytic stability analysis is not feasible, so we perform a numerical stability analysis. In particular, we use $g=1.3$, 1.2, 1.05, and 0.993 for $M=1$, 5, 20, and 50, respectively, where $g \lesssim g_c$ in all cases.

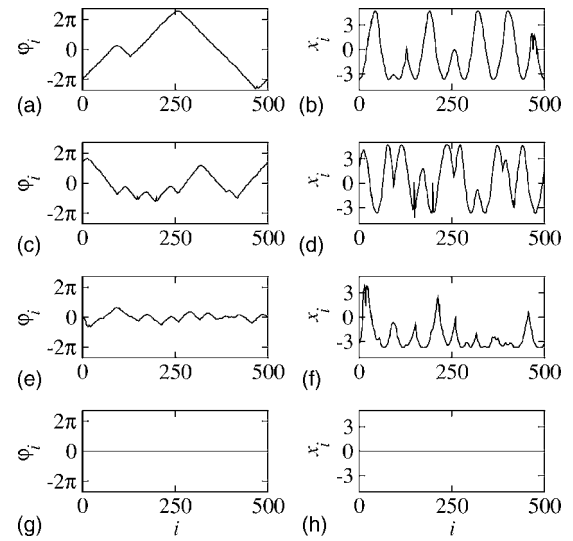

FIG. 2. Snapshots of $\varphi_i(t)$ and $x_i(t)$ for $t=8400$ and for four different values of M (the number of shortcuts): (a, b) $M=1$ and $g=1.3$, (c, d) $M=5$ and $g=1.2$, (e, f) $M=20$ and $g=1.05$, and (g, h) $M=50$ and $g=0.993$, the system diverges for $g=0.994$.

For $M \leqslant 20$, the eigenmode associated with the largest eigenvalue is unstable ($g\lambda_N > K_c$), but all other eigenmodes are stable ($g\lambda_i < K_c$ for all $i<N$), for the two largest eigenvalues are $(\lambda_N, \lambda_{N-1})=(3.34, 3.18)$, (3.83,3.37), and (4.04,3.85) for $M=1$, 5 and 20, respectively. When $M=50$, all eigenmodes are stable even for $g \lesssim g_c$, leading to flat surfaces in both snapshots of $\varphi_i(t)$ and $x_i(t)$ (see Fig. 2). As the number of shortcuts is increased, the ring network becomes effectively more random and synchronized motion is observed. In this case, the parameter interval for desynchronized waves shrinks. The phenomenon persists even when the Rössler oscillators are made slightly different.

As the network loses the degree of regularity by increasing the number of random shortcuts, desyncrhonization wave pattern disappears gradually. For random and scale-free networks, no ordered wave patterns have been observed. For instance, we have generated a scale-free network of 500 nodes and average connectivity $\langle k \rangle = 4$ by using the method in Barabási and Albert [9]. No ordered wave pattern is observed in the network for $g \lesssim g_c$. We have also generated a random network of 500 nodes and $\langle k \rangle = 4$ by using the method in Ref. [20] and have found a similar behavior. These results show that regularity in the connectivity of the network is needed for ordered desynchronized wave patterns.

III. PHASE EVOLUTION EQUATION FOR DESYNCHRONIZED WAVE PATTERN

The observed desynchronization wave patterns in Sec. II can be explained by considering the evolution of phase of each oscillator near the critical value g_c. Let C denote the stable closed orbit corresponding to $\mathbf{x}$. The phase φ of an isolated oscillator increases with time monotonically [21]

$$\frac{d\varphi}{dt} = \omega_0, \quad \mathbf{x} \in C, \tag{5}$$

where ω_0 is the frequency. Now assume that the velocity field is perturbed. We write

$$\frac{d\mathbf{x}}{dt} = \mathbf{F}(\mathbf{x}) + \epsilon \mathbf{p}(\mathbf{x}), \tag{6}$$

where $\mathbf{p}(\mathbf{x})$ denotes the perturbation and ϵ is an indicator of the smallness of $\mathbf{p}$. The small perturbation leads to slight deviation of the period of the oscillator but the periodic motion of the oscillator persists. To find the small change in the period to the lowest order ϵ, we write Eq. (6) as

$$\frac{d\varphi(\mathbf{x})}{dt} = \mathbf{Z}(\varphi)\frac{d\mathbf{x}}{dt} = \mathbf{Z}(\varphi) \cdot [\mathbf{F}(\mathbf{x}) + \epsilon \mathbf{p}(\mathbf{x})], \tag{7}$$

where $\mathbf{Z}(\varphi) = \mathrm{grad}_{\mathbf{x}}\, \varphi$. Since C is a stable orbit, the condition $\mathbf{Z}(\varphi) \cdot \mathbf{F}(\mathbf{x}) = \omega_0$ is satisfied. We obtain

$$\frac{d\varphi(\mathbf{x})}{dt} = \omega_0 + \epsilon \mathbf{Z}(\varphi) \cdot \mathbf{p}(\mathbf{x}). \tag{8}$$

Suppose that in the ring network, each link connecting two neighboring oscillators has a small coupling constant that is a random number between D_0 and D_1 ($D_1 > D_0 > 0$).

The perturbation $\mathbf{p}$ at oscillator i due to the network connection is given by

$$\mathbf{p}(\mathbf{x}_i) = ga_{ji}(\mathbf{x}_j - \mathbf{x}_i) + ga_{ik}(\mathbf{x}_k - \mathbf{x}_i) = gD_0(\mathbf{x}_j + \mathbf{x}_k - 2\mathbf{x}_i) + ga'_{ji}(\mathbf{x}_j - \mathbf{x}_i) + ga'_{ik}(\mathbf{x}_k - \mathbf{x}_i), \quad (9)$$

where $j=i-1$, $k=i+1$, $a_{ji}=D_0+a'_{ji}$, $a_{ik}=D_0+a'_{ik}$, a_{ji} and a_{ik} are random coupling constants, and g is a global coupling constant. In the continuum limit we have

$$\mathbf{p}(\mathbf{x}) = \tilde{D}\frac{\partial^2 \mathbf{x}}{\partial \xi^2} - c_1\frac{\partial \mathbf{x}}{\partial \xi} + c_2\frac{\partial \mathbf{x}}{\partial \xi} = \tilde{D}\frac{\partial^2 \mathbf{x}}{\partial \xi^2} + \tilde{c}\frac{\partial \mathbf{x}}{\partial \xi}, \quad (10)$$

where $\tilde{D}=gD_0$, $c_1=ga'_{ji}$, $c_2=ga'_{ik}$, and $\tilde{c}=c_2-c_1$. Equation (10) can be rewritten as

$$\mathbf{p}(\mathbf{x}_\xi) = \tilde{D}\mathbf{\Pi}(\varphi)\frac{\partial^2 \varphi}{\partial \xi^2} + \tilde{D}\mathbf{\Upsilon}(\varphi)\left(\frac{\partial \varphi}{\partial \xi}\right)^2 + \tilde{c}\mathbf{\Pi}(\varphi)\frac{\partial \varphi}{\partial \xi}, \quad (11)$$

where $\mathbf{\Pi}(\varphi)=d\mathbf{x}(\varphi)/d\varphi$ and $\mathbf{\Upsilon}(\varphi)=d^2\mathbf{x}(\varphi)/d\varphi^2$. Inserting Eq. (11) in Eq. (8), we get a partial differential equation

$$\frac{\partial \varphi(\mathbf{x})}{\partial t} = \omega_0 + c\Omega^{(1)}(\varphi)\frac{\partial \varphi}{\partial \xi} + D\Omega^{(1)}(\varphi)\frac{\partial^2 \varphi}{\partial \xi^2} + D\Omega^{(2)}(\varphi)\left(\frac{\partial \varphi}{\partial \xi}\right)^2, \quad (12)$$

where $c=\epsilon\tilde{c}$, $D=\epsilon\tilde{D}$, and $\Omega^{(1)}(\varphi)=\mathbf{Z}(\varphi)\cdot\mathbf{\Pi}(\varphi)$ and $\Omega^{(2)}(\varphi)=\mathbf{Z}(\varphi)\cdot\mathbf{\Upsilon}(\varphi)$ are T-periodic functions. In order to obtain the average values for $\Omega^{(1)}$ and $\Omega^{(2)}$, we introduce a phase disturbance variable ψ according to $\varphi=\omega_0 t+\psi$ and write Eq. (12) as

$$\frac{\partial \psi}{\partial t} = c\Omega^{(1)}(\omega_0 t+\psi)\frac{\partial \psi}{\partial \xi} + D\Omega^{(1)}(\omega_0 t+\psi)\frac{\partial^2 \psi}{\partial \xi^2} + D\Omega^{(2)}(\omega_0 t+\psi)\left(\frac{\partial \psi}{\partial \xi}\right)^2. \quad (13)$$

Since ψ is a slow variable, it hardly changes during the period T and thus Eq. (13) can be time averaged. After averaging the periodic coefficients over the period T, we have

$$\frac{\partial \psi}{\partial t} = \omega\frac{\partial \psi}{\partial \xi} + \nu\frac{\partial^2 \psi}{\partial \xi^2} + \lambda\left(\frac{\partial \psi}{\partial \xi}\right)^2 \quad (14)$$

and

$$\frac{\partial \varphi}{\partial t} = \omega_0 + \omega\frac{\partial \varphi}{\partial \xi} + \nu\frac{\partial^2 \varphi}{\partial \xi^2} + \lambda\left(\frac{\partial \varphi}{\partial \xi}\right)^2, \quad (15)$$

where $\omega=c\nu/D$ is a random number depending on the site ξ, ν, and λ are constants defined by

$$\nu = \frac{D}{T}\int_0^T \Omega^{(1)}(\omega_0 t)dt$$

and

$$\lambda = \frac{D}{T}\int_0^T \Omega^{(2)}(\omega_0 t)dt.$$

When shortcuts are added to the network so that it becomes small-world, the perturbation at oscillator i is changed

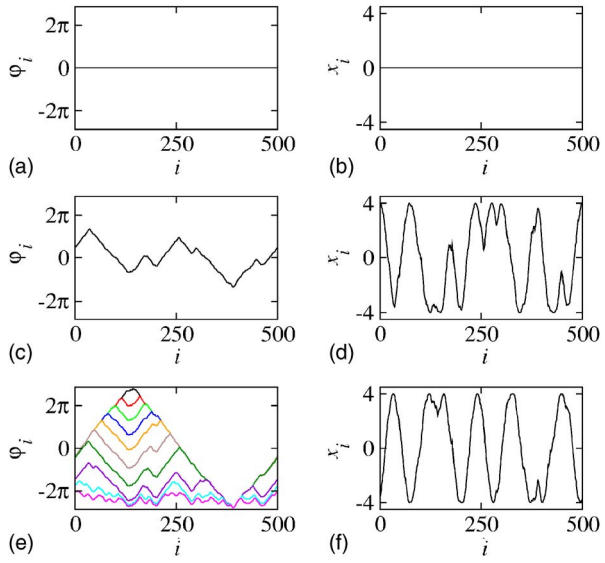

FIG. 3. (Color online) Snapshots of numerical solution of Eq. (15) without shortcuts for $t=0$ (a, b), $t=100$ (c, d), $t=8400$,700, 600, 500, 400, 275, 150, 50, 20, and 10 from top to bottom (e), and $t=8400$ (f). Left-hand panels, phase surface $\varphi_i(t)$. Right-hand panels, the corresponding x_i profile.

to $\mathbf{p}'(\mathbf{x}_i)=\mathbf{p}(\mathbf{x}_i)+\mathbf{p}_0(\mathbf{x}_i)$ from $\mathbf{p}(\mathbf{x}_i)$, where $\mathbf{p}_0(\mathbf{x}_i)=\Sigma_l a_{il}(\mathbf{x}_l-\mathbf{x}_i)$ is the new perturbation term due to the shortcuts and the sum is over all shortcuts that end at site i. By using the method used to obtain Eq. (15), we have, approximately,

$$\epsilon\mathbf{Z}(\varphi)\cdot\mathbf{p}'(\mathbf{x}_i) = \omega_s\sum_l[\varphi(l)-\varphi(i)], \quad (16)$$

where ω_s is a random number that has different value for each shortcut. In the continuum limit, the last term in Eq. (16) can be written as $\omega_s\int_\zeta[\varphi(\zeta)-\varphi(\xi)]d\zeta \approx \omega_s\int_\zeta(\partial\varphi/\partial\xi)d\zeta$, where i and $l(=i+a)$ are replaced with ξ and ζ, a constant a is set to 1, and $\int_\zeta d\zeta$ means a summation over site l. We then obtain the general equation for the evolution of phase in the small-world type of oscillator network,

$$\frac{\partial \varphi(\xi,t)}{\partial t} = \omega_0 + \omega(\xi)\frac{\partial \varphi}{\partial \xi} + \nu\frac{\partial^2 \varphi}{\partial \xi^2} + \lambda\left(\frac{\partial \varphi}{\partial \xi}\right)^2 + \omega_s(\zeta,\xi)\int_\zeta \frac{\partial \varphi}{\partial \xi}d\zeta. \quad (17)$$

Equation (17) is a general type of KPZ equation [22,23]. For $w_s=0$, Eq. (17) is similar to quenched KPZ equation. In the quenched KPZ equation, the KPZ nonlinear term $\lambda(\frac{\partial\varphi}{\partial\xi})^2$ makes $\varphi(\xi)$ surface rough, similar to the behavior in Fig. 1(e)[24–26].

To test the use of Eq. (17) to describe the desynchronized wave phenomenon in oscillator networks, we first consider the case of $\omega_s=0$ so that the network is regular. We set parameter values (somewhat arbitrarily) to be $\nu=0.05$, $\lambda=-0.4$, ω a random number between -2 and 2, and solve Eq. (17) by using the standard finite-difference method with $N=500$ spatial sites (the number of oscillators in the network). Figures 3(a), 3(c), and 3(e) show the phase surface at a number of different times. The dynamical variable of the

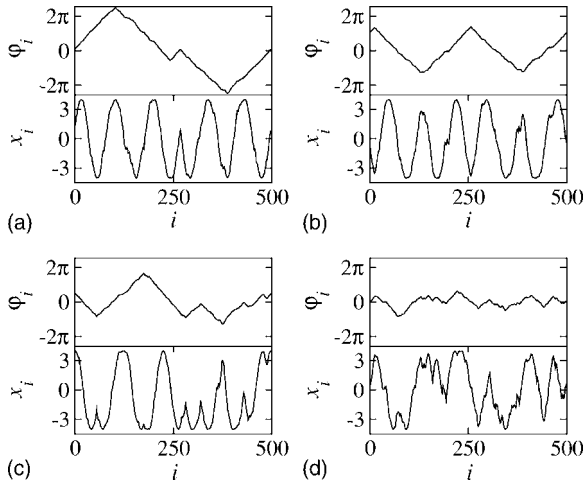

FIG. 4. Snapshots of the solution of Eq. (17) with shortcuts for $t=8400$ (steady state) for four difference cases: (a) one randomly placed shortcut, (b) one shortcut connecting the node with the lowest frequency and its diametrical node, (c) five randomly placed shortcuts, and (d) 20 randomly placed shortcuts.

oscillator can be obtained from the phase variable by $x(\xi,t)=A\ \sin[\varphi(\xi,t)]$, where we choose $A=4$ (approximately the amplitude of the periodic oscillation of the Rössler system). Some snapshots of $x(\xi,t)$ are shown in Figs. 3(b), 3(d), and 3(f). We observe the emergence of an ordered desynchronization wave pattern. To take into account shortcuts, we set ω_s to be random values in the interval [1.5,2.5] in Eq. (17). Figures 4(a)–4(d) show the phase surface (upper panel) and the x-profile (lower panel) for four cases where (a) one shortcut is randomly placed, (b) one shortcut is placed which connects a node and its diametrical node, (c, d) five and 20 shortcuts are placed randomly, respectively. We see that there are increasingly more local minima in the steady-state phase surface as the number of shortcuts is increased, eventually destroying the ordered wave pattern.

IV. CONCLUSION

In summary, we have uncovered a phenomenon concerning desynchronization wave patterns that typically appear in regular networks with random coupling: a small number of shortcuts, which make the network small-world, can actually destroy ordered wave patterns which disappear gradually as the number of shortcut is increased, i.e., as the network regularity deteriorates. We have derived a general KPZ type of equation to account for this phenomenon. Our results show that ordered desynchronized wave patterns require a certain degree of regularity in the network. Ordered wave patterns are important spatiotemporal dynamical phenomena that are potentially relevant to a number of fields. Our finding suggests that network connecting topologies can have a drastic effect on these wave patterns, a topic that deserves further attention.

ACKNOWLEDGMENTS

This work is supported by NSF under Grant No. ITR-0312131 and by AFOSR under Grants No. FA9550-06-1-0024 and F49620-01-01-0317.

[1] M. Barahona and L. M. Pecora, Phys. Rev. Lett. **89**, 054101 (2002).
[2] X. F. Wang and G. Chen, Int. J. Bifurcation Chaos Appl. Sci. Eng. **12**, 187 (2002).
[3] T. Nishikawa, A. E. Motter, Y.-C. Lai, and F. C. Hoppensteadt, Phys. Rev. Lett. **91**, 014101 (2003).
[4] A. E. Motter, C. Zhou, and J. Kurths, Europhys. Lett. **69**, 334 (2005); Phys. Rev. E **71**, 016116 (2005).
[5] L. Donetti, P. I. Hurtado, and M. A. Muñoz, Phys. Rev. Lett. **95**, 188701 (2005).
[6] K. Park, Y.-C. Lai, S. Gupte, and J.-W. Kim, Chaos **16**, 015105 (2006).
[7] L. Huang, K. Park, Y.-C. Lai, L. Yang, and K. Yang, Phys. Rev. Lett. **97**, 164101 (2006).
[8] D. J. Watts and S. H. Strogatz, Nature (London) **393**, 440 (1998).
[9] R. Albert and A.-L. Barabási, Rev. Mod. Phys. **74**, 47 (2002).
[10] S. N. Dorogovtsev and J. F. F. Mendes, Adv. Phys. **51**, 1079 (2002).
[11] M. E. J. Newman, SIAM Rev. **45**, 167 (2003).
[12] S. N. Dorogovtsev and J. F. F. Mendes, *Evolution of Networks: From Biological Networks to the Internet and WWW* (Oxford University Press, Oxford, 2003).
[13] A.-L. Barabási and R. Albert, Science **286**, 509 (1999).
[14] L. M. Pecora and T. L. Carroll, Phys. Rev. Lett. **80**, 2109 (1998).
[15] A. Pikovsky, M. G. Rosenblum, and J. Kurths, *Synchronization: A Universal Concept in Nonlinear Sciences* (Cambridge University Press, Cambridge, 2001).
[16] See, for example, E. Mosekilde, Y. Maistrenko, and D. Postnov, *Chaotic Synchronization: Applications to Living Systems* (World Scientific, Singapore, 2002).
[17] See, for example, R. Roy and K. S. Thornburg, Phys. Rev. Lett. **72**, 2009 (1994).
[18] See, for example, W. Wang, I. Z. Kiss, and J. L. Hudson, Chaos **10**, 248 (2000).
[19] J. G. Restrepo, E. Ott, and B. R. Hunt, Phys. Rev. Lett. **93**, 114101 (2004).
[20] Z. Liu, Y.-C. Lai, N. Ye, and P. Dasgupta, Phys. Lett. A **303**, 337 (2002).
[21] Y. Kuramoto, *Chemical Oscillations, Waves, and Turbulence* (Springer-Verlag, Berlin, 1984).
[22] M. Kardar, G. Parisi, and Y.-C. Zhang, Phys. Rev. Lett. **56**, 889 (1986).
[23] J. M. Kim and J. M. Kosterlitz, Phys. Rev. Lett. **62**, 2289 (1989).
[24] K. Sneppen, Phys. Rev. Lett. **69**, 3539 (1992).
[25] H. Jeong, B. Kahng, and D. Kim, Phys. Rev. E **59**, 1570 (1999).
[26] K. Park, H.-J. Kim, and I.-M. Kim, Phys. Rev. E **62**, 7679 (2000).